CHEMICAL ENGINEERING TRANSACTIONS
VOL. 103, 2023
A publication of AIDIC
The Italian Association of Chemical Engineering
Online at www.cetjournal.it
Guest Editors: Petar S. Varbanov, Panos Seferlis, Yee Van Fan, Athanasios Papadopoulos

ISBN 979-12-81206-02-1; **ISSN** 2283-9216
DOI: 10.3303/CET23103081

Numerical Simulation of Blade-Shaped Riblets Using LES-Based Methods

Chris Bliamis[a], Zinon Vlahostergios[b,*], Dimitrios Misirlis[c], Kyros Yakinthos[a]

[a] Laboratory of Fluid Mechanics and Turbomachinery, Department of Mechanical Engineering, Aristotle University of Thessaloniki, 54124 Thessaloniki, Greece
[b] Laboratory of Fluid Mechanics and Hydrodynamic Machines, Department of Production and Management Engineering, Democritus University of Thrace, 67100 Xanthi, Greece
[c] Department of Mechanical Engineering, International Hellenic University, 62124 Serres, Greece
zvlachos@pme.duth.gr

Passive flow control techniques are widely implemented in many areas of fluid mechanics and aerodynamics, aiming at permanently altering the flow field to suppress undesired phenomena or enhance performance. Among many passive flow control techniques proposed for aeronautical applications, the microgroove geometries called riblets are especially promising in reducing an aircraft's skin friction drag by altering the boundary layer characteristics in the near-the-wall region. In the present study, various blade-shaped riblets designed for application on an Unmanned Aerial Vehicle (UAV), are examined and evaluated through both Large Eddy Simulations (LES), as well as hybrid Embedded LES (ELES) computations. The different riblet geometries are simulated at zero-pressure gradient flow, their drag-reducing potential is identified, and their near-wall behaviour is examined. The use of ELES as a simulation method for riblet simulation is also evaluated. Concludingly, the riblets with equal width-to-height ratio ($s/h = 1$) demonstrate the best drag reducing results, while those with the largest width ($s/h = 2$) exhibit very poor performance and exceptionally high wall shear stresses. Finally, the hybrid ELES simulations are quantitatively similar with those performed using purely LES but result in higher absolute drag force values, due to the RANS-LES interface interference with the flow development.

1. Introduction

Riblets have been a promising and actively studied passive, for the past few decades, flow control method that can reduce the viscous drag in turbulent wall-bounded flows. The usefulness of such a method is highly evident in the case of civil aircraft, where the friction-related drag component can account for as much as 50 % of the overall aircraft drag (Viswanath, 2002). More specifically, riblets are streamwise-aligned micro-grooved geometries (in the order of 100-1,000 μm) which affect the near wall region of the boundary layer with three distinct mechanisms: (a) by elevating upwards the cross-flow motion in their crests and displacing streamwise vortices and streaks away from the wall, (b) by weakening the near-wall turbulence regeneration cycle and (c) by dampening the spanwise flow fluctuations (Bannier et al., 2015). However, they also amplify the two-dimensional Tollmien–Schlichting waves, and inappropriately designed or placed riblets can result in a drag increase as they promote the laminar to turbulent boundary layer transition (Klumpp et al., 2010a).
The initial research studies of riblets were focused on experimental investigations where the various riblet geometries (mostly triangular and sinusoidal) were studied in channel flows. European researchers made extensive use of oil tunnel experiments to identify the importance of the riblet shape and size, as well as that of their tip sharpness (Bechert et al., 1997). Similarly in the USA, riblets were studied in various wind tunnel facilities, employing aerodynamic force balance and hot-wire measurements (Walsh and Anders, 1989). In these early experimental works, the viscous drag reduction from riblets was measured to be in the range of 4-8 % for two-dimensional flows at zero or mild pressure gradients. The use of riblets as a drag reduction method has been assessed at high Reynolds number conditions and Mach numbers between 0.3 and 0.7, in a number of flight tests by Boeing (McLean et al., 1987), Airbus (Coustols and Savill, 1992), NASA (Walsh et al., 1989) and

Paper Received: 26 April 2023; Revised: 26 June 2023; Accepted: 28 July 2023
Please cite this article as: Bliamis C., Vlahostergios Z., Misirlis D., Yakinthos K., 2023, Numerical Simulation of Blade-Shaped Riblets Using LES-Based Methods, Chemical Engineering Transactions, 103, 481-486 DOI:10.3303/CET23103081

more recently JAXA (Kurita et al., 2020). In these flight tests, the viscous drag reduction was measured to be around 6 %, and at the same value level as the corresponding wind tunnel and DNS measurements.

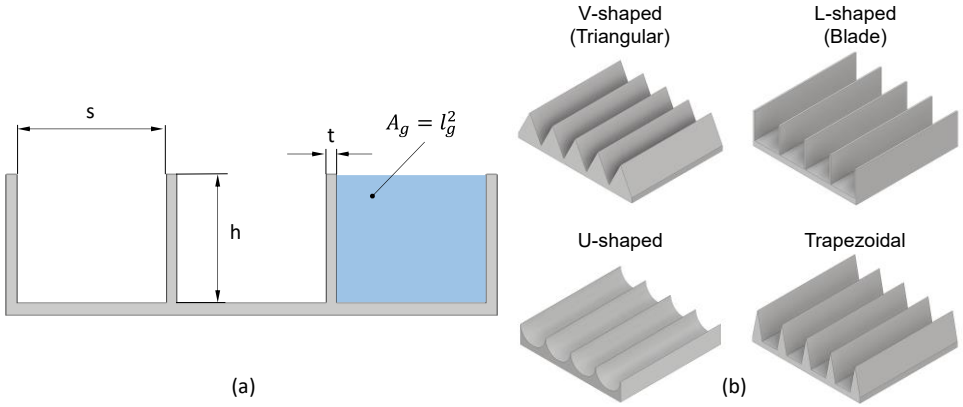

Figure 1: (a) Typical riblet geometries and (b) blade-shaped riblets with basic dimensions

The extremely small dimensions of riblets prohibited the detailed experimental investigation of the complex flow structures that develop within the riblet grooves, and towards that aim, researchers have resulted in the employment of Direct Numerical Simulation (DNS) methods (Choi et al., 1993). However, DNS is currently unfeasible for high-Reynolds number flows and complex geometries, and several works involve the use of Large Eddy Simulations (LES) methods to predict the performance of riblets on flat plates with zero (ZPG) and adverse pressure gradient (APG) (Klumpp et al., 2010b) and on airfoils (Zhang et al., 2018), even though these methods are still extremely more resource-demanding compared to typical industrial Reynolds Averaged Navier-Stokes (RANS) analyses.

To overcome the high computational cost of such high-fidelity CFD simulations, surrogate modelling techniques have been used to model the effect of riblets in more complex geometries while only solving the RANS equations. Firstly, the model proposed by Mele and Tognaccini (2012), models the riblets as a singular roughness problem and, more specifically, does so by altering the original boundary condition for the specific turbulence dissipation rate ω. This model has been successfully implemented in cases related to airfoils (Bliamis et al., 2020), regional airliners (Catalano et al., 2018), and UAVs (Bliamis et al., 2022), with the riblet geometry being presented through the square root of the groove cross-section (l_g). Also, the surrogate model by Mele and Tognaccini (2018) employs a slip-length boundary condition to model the effect of riblets and induce a shift in the log-law near the wall. Though both surrogate models can be used to model riblets adequately, the slip-length model has the additional advantage of incorporating the effect of riblet alignment with the flow and is not restricted solely to ω-based turbulence models, with the main drawback being the complexity of its implementation to the CFD solver.

This work focuses on the computational investigation of blade-shaped riblets, designed in the framework of the "RADAERO - Innovative Composite Materials for the Drag and Electromagnetic Signature Reduction for Applications in Aviation" project, in which riblets and innovative metamaterial absorbers will be applied on an Unmanned Aerial Vehicle (UAV). The main aim of the work is to examine both the riblet shape as a design parameter, as well as the use of different numerical methods. Two different methods are employed, namely the Large Eddy Simulation (LES) and the hybrid Embedded Large Eddy Simulation (ELES). The novel approach of employing the ELES method for riblet simulation is evaluated by comparing its results with those obtained from the pure LES. Additionally, the riblet geometry is another examined parameter, with three different blade-shaped riblets being investigated. In all these cases, the groove cross-sectional area (A_g) is maintained constant, while different width-to-height ratios (s/h) are examined (i.e., 0.5, 1 and 2). To validate the accuracy of the employed numerical methods, a set of triangular riblets are also simulated with LES and ELES, and the results are compared against the published DNS data of Choi et al. (1993).

2. Tools and Methods

2.1 Riblet specimens

In the framework of the RADAERO, a number of blade-shaped riblet geometries have been designed and manufactured by the consortium partners. In the present work, these specimens are investigated numerically, with the methods presented in the next chapter, but they will also be examined experimentally in a wind tunnel setup in the near future. Three different blade-shaped riblets were manufactured, where the groove cross-

sectional area (A_g) is kept constant at (and also the l_g) and only the width (s) and height (h) is altered. One set of triangular riblets is also examined to validate the LES-based methods with the already published DNS results of Choi et al. (1993). The basic dimensions of the examined riblets are presented below in Table 1.

Table 1: Basic geometric characteristics of examined riblets

Case #	Type	s [μm]	h [μm]	l_g [μm]	α [deg]	s/h	t/h
B-1	Blade	1,500	750	1,060	-	2	0.1
B-2	Blade	1,060	1,060	1,060	-	1	0.07
B-3	Blade	750	1,500	1,060	-	0.5	0.05
T-1	Triangular	340	170	170	60	2	-

2.2 CFD methodology

To simulate the flow field in the near-wall region when riblets are applied, two high-fidelity numerical methods are employed, namely Large Eddy Simulations (LES) and Embedded Large Eddy Simulations (ELES), the latter of which is a hybrid zonal RANS-LES method.

For all analyses, the required computational meshes are generated using the BETA ANSA pre-processing software (v23.1.0, Root, Switzerland), are structured, and consist solely of hexahedral cells. In each riblet case examined, the computational mesh is slightly different due to the variation in h and s, which in turn result in a different number of cells in the y and z directions (presented in Table 2). In the computational domain, 8 riblets are included, with 12 (B-3) and 16 (B-1, B-2) cells being used for the discretisation of each one's width (s) and 2 cells for their thickness (t). The mesh is refined in the region near the riblet tips and becomes coarser towards the middle of their width (z-direction) and towards the bottom of their valley. This is presented for the B-2 mesh in Figure 2a. An appropriate first layer height is enforced in the overall riblet-covered area, ensuring that everywhere the y^+ is below 1. The height of the computational domain is 2δ, the streamwise length (L_x) is $\pi\delta$ and the spanwise length (L_z) is 0.908δ. In each case, the Reynolds number based on the half channel width δ is different, since the mean velocity U_{AVG} is maintained constant at 15 m/s. This velocity is defined as $U_{AVG} = Q/A$ and corresponds to the wind tunnel conditions in which the riblets will be experimentally investigated in future work.

Table 2: Blade riblets grid and simulation parameters

Case #	N_x	N_y	N_z	Total cells	Re_δ
B-1	60	100	144	864,000	14,300
B-2	60	109	144	941,760	10,600
B-3	60	121	112	813,120	8,000

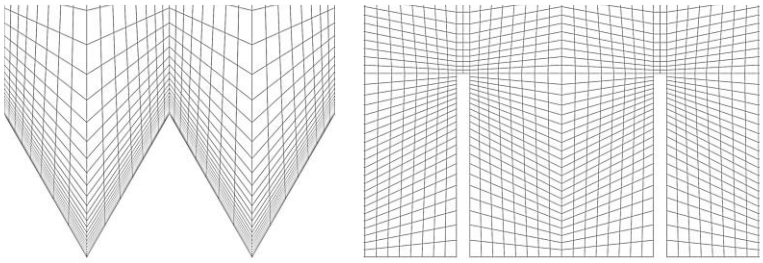

(a) (b)

Figure 2: Detail of the computational meshes in the riblet region for (a) the B-2 case and (b) the T-1 case

All simulations are performed using the ANSYS Fluent 2020R2 (Academic Multiphysics Campus Solution) software (Canonsburg, PA, USA) and, more specifically, with the coupled pressure-based solver. In the pure LES analyses, the filtered time-dependent Navier-Stokes are solved in the whole computational domain, with the Smagorinsky-Lilly model being utilised for the subgrid-scale (SGS) modelling. The bounded central differencing scheme is used for the discretisation of the momentum equations, and the bounded second-order implicit formulation for the temporal discretisation. In the Embedded LES analyses, the computational domain is separated into two distinct zones (Figure 3b), the LES subdomain in the region near the riblets (up to a height of $2.5h$) and the RANS subdomain above that. In the first subdomain, the filtered time-dependent Navier-Stokes equations are solved, similar to the pure LES analyses. In the RANS subdomain, the unsteady RANS equations are solved, with second-order upwind schemes for the spatial discretisation of the transport equations and the

bounded second-order implicit formulation for the temporal discretisation, and they are closed with the adoption of the k-ω SST turbulence model. Between the two subdomains, a RANS-LES interface exists, where the modeled turbulence kinetic energy is converted into resolved energy, using the Spectral Synthesizer method.

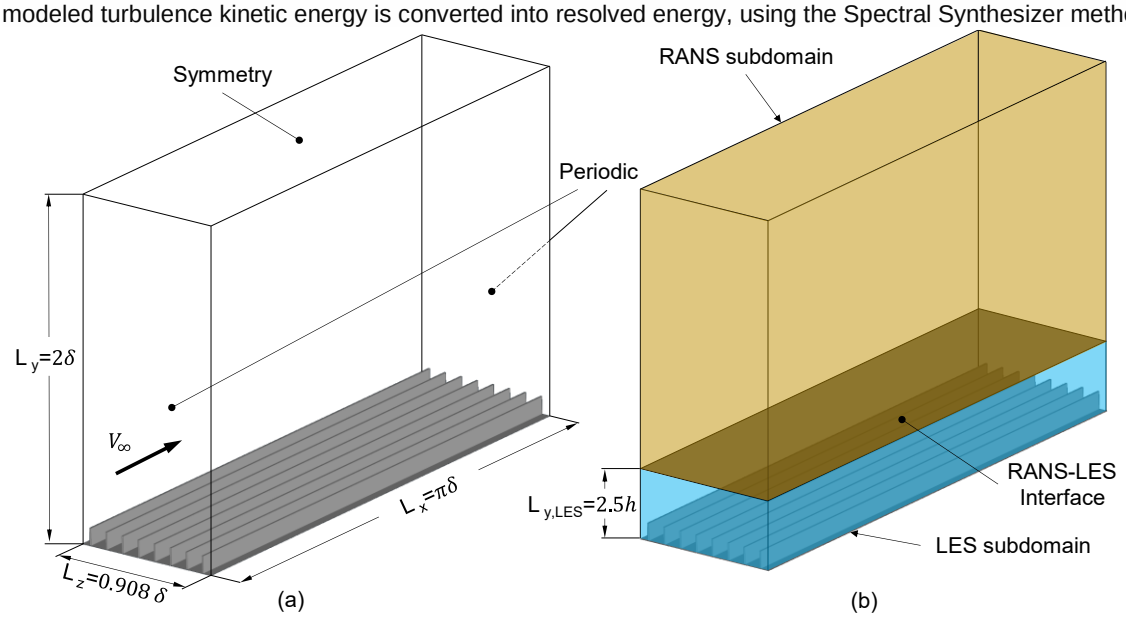

Figure 3: (a) Dimensions of the computational domain with boundary conditions and (b) ELES computational domains subdivision

To ensure the accuracy of the employed methods, the flow over the triangular T-1 riblets is simulated with both LES and ELES, as described above, and the results are compared with those of Choi et al. (1993) obtained through DNS analysis. Specifically, the T-1 riblets are modelled in channel flow with a Re_δ equal to 2,800. In these analyses, the upper boundary of the computational domain consists of a solid flat plate surface, and a cell spacing similar to that on the riblet side is used. In the ELES analysis, a second LES subdomain exists right below the solid flat plate with a height of 2.5 h. The analyses showed a drag reduction of about 7.0 % and 6.8 %, with the LES and ELES methods. These are in quite good agreement with the DNS results (6.4 %) of Choi et al. (1993). However, it is noted that the ELES method results in significantly higher wall shear stress values.

3. Results

In both the LES and Embedded LES analyses, a similar trend is observed, with the B-1 and B-3 riblets demonstrating higher drag coefficient values than the B-2 riblets. More specifically, the drag coefficient of B-1 is significantly higher due to the wider groove width (s) which does not activate the drag-reducing mechanisms of riblets and has the opposite effect of leading to increased wall shear stresses in the riblet valleys. In Figure 4, the wall shear stresses, along with the developed vortical structures, are presented from the ELES simulations.

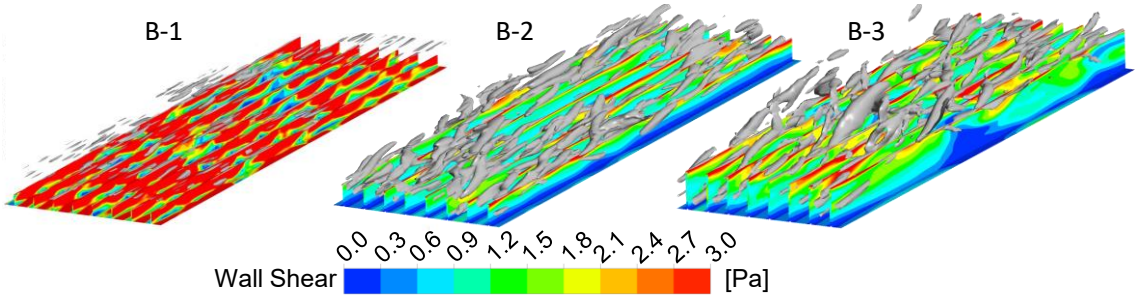

Figure 4: Wall shear stress distribution and near riblet vortical structures from the ELES simulations

The increased wall shear stress behavior in the ELES analyses is observed in the blade-shaped riblets as well (Table 3). This behavior can be attributed to the position of the RANS-LES interface above the riblets and its

associated interference between the modelled and resolved scales. In Figure 5, the streamwise vorticity of the B-2 riblets, in position $L_x/2$ is presented, and it is observed that the RANS-LES interface dampens the flow development in the normal direction and restrains the development of vortical structures. This is also evident when the pure LES results of B-3 riblets (Figure 6) are compared against those of Figure 4 (B-3), where vortical structures are greater in number, smaller in size, and are maintained closer to the riblets.

Table 3: Drag coefficients of the examined riblets with LES and ELES simulations

Method	$C_{d,B-1}$	$C_{d,B-2}$	$C_{d,B-3}$
LES	0.0178	0.0067	0.0079
ELES	0.0484	0.0174	0.0328

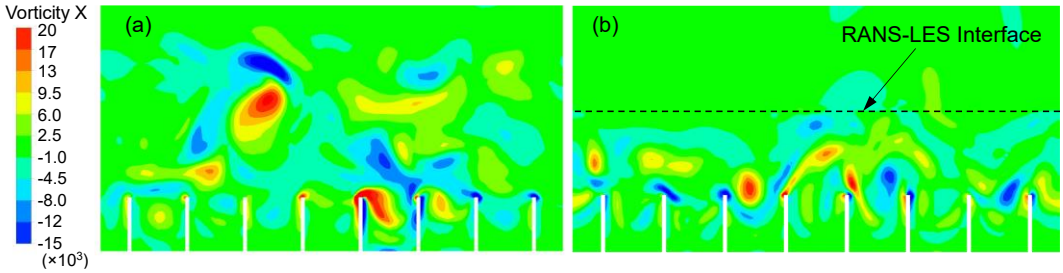

Figure 5: Streamwise vorticity contours near the B-2 riblets from (a) LES and (b) ELES simulations

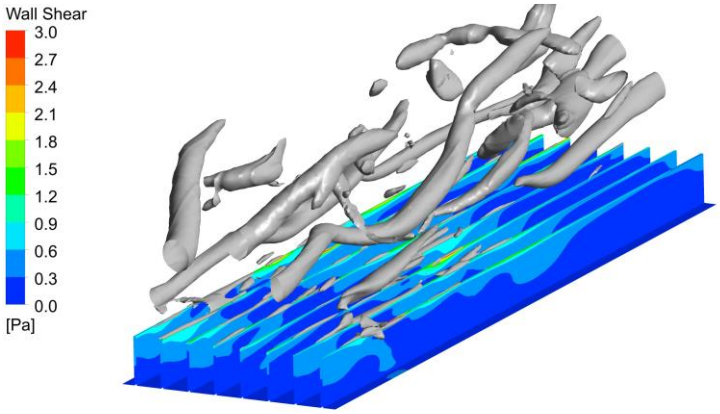

Figure 6: Wall shear stress distribution and near riblet vortical structures from the LES simulations of B-3 riblets

4. Conclusions

In this work, the numerical simulation of blade-shaped riblets using high-fidelity CFD methods is presented. The use of both LES and hybrid RANS-LES methods (Embedded LES), is examined, and important remarks regarding their performance are made. The novel employment of a hybrid zonal method (ELES) is evaluated as a possible method for riblet simulation. Additionally, three different blade-shaped riblet geometries are simulated with the above mentioned numerical methods. These riblets feature the same square root of the groove cross-section (l_g), which is a very good indicator of their performance, but differ in their height and width (h, s). Both LES and Embedded LES simulations showed that the riblets of equal height and width (B-2) demonstrate the best performance, though those with an s/h ratio of 0.5 are also quite close (B-3). The riblets with double width compared to height (B-1) demonstrate significantly worse performance, since the groove width is not adequate to interfere with the developed vortical structures, which leads to increased wall shear stresses in the riblet valleys. Regarding the different simulation methods, pure LES provides the optimal results, with significantly smaller friction drag values. In the Embedded LES, the presence of the RANS-LES interface interferes with the development of vortical structures, and higher wall shear stresses are developed. In future work, a parametric investigation into the effect of the RANS-LES interface positioning, with different riblet heights, will be conducted.

Nomenclature

t – riblet thickness, m

h – riblet height, m

s – riblet width, m
A_g – riblet groove cross-section, m^2
l_g – square root of riblet groove cross-section, m
U_{AVG} – mean flow velocity, m/s
a – riblet tip angle, deg
δ – channel half-width, m

Acknowledgments

This work was implemented within the project “RADAERO-Innovative Composite Materials for the Drag and Electromagnetic Signature Reduction for Applications in Aviation” (project code: Τ6ΥΒΠ-00042), which was financially supported by the European Regional Development Fund, Partnership Agreement for the Development Framework (2014–2020), co-funded by Greece and the European Union in the framework of the OPERATIONAL PROGRAMME: “Competitiveness, Entrepreneurship and Innovation 2014–2020 (EPAnEK)”, Nationwide Action: “Industrial Materials”.
The authors would like to acknowledge that the results presented in this work have been produced using the Aristotle University of Thessaloniki (AUTh) High Performance Computing Infrastructure and Resources.
The authors Chris Bliamis and Kyros Yakinthos are also affiliated with the UAV-iRC of the Center for Interdisciplinary Research and Innovation, Aristotle University of Thessaloniki Greece. The authors Zinon Vlahostergios and Dimitrios Misirlis are also affiliated with the Laboratory of Fluid Mechanics and Turbomachinery, Department of Mechanical Engineering, Aristotle University of Thessaloniki, Greece.

References

Bannier A., Garnier É., Sagaut P., 2015, Riblet Flow Model Based on an Extended FIK Identity, Flow Turbulence and Combustion, 95, 351–376, DOI:10.1007/s10494-015-9624-2.
Bechert D., Bruse M., Hage W., van der Hoeven J., Hoppe G., 1997, Experiments on drag-reducing surfaces and their optimization with an adjustable geometry, Journal of Fluid Mechanics, 338, 59–87, DOI:10.1017/S0022112096004673.
Bliamis C., Vlahostergios Z., Misirlis D., Yakinthos K., 2020, Modeling Surface Riblets Skin Friction Reduction Effect with the Use of Computational Fluid Dynamics, Chemical Engineering Transactions, 81, 595-600, DOI:10.3303/CET2081100.
Bliamis C., Vlahostergios Z., Misirlis D., Yakinthos K., 2022, Numerical Evaluation of Riblet Drag Reduction on a MALE UAV, Aerospace, 9, 218 DOI:10.3390/aerospace9040218.
Catalano P., de Rosa D., Mele B., Tognaccini R., Moens F., 2018, Effects of riblets on the performances of a regional aircraft configuration in NLF conditions, AIAA Aerospace Sciences Meeting 2018, 1-16, DOI:10.2514/6.2018-1260.
Choi H., Moin P., Kim J., 1993, Direct numerical simulation of turbulent flow over riblets, Journal of Fluid Mechanics, 255, 503–539, DOI:10.1088/1468-5248/3/1/007.
Coustols E., Savill A., 1992, Turbulent Skin-Friction Drag Reduction By Active and Passive Means, AGARD, Report 786 part 1, Seine, France, 1992, pp.8.1–8.53.12.
Klumpp S., Meinke M., Schröder W., 2010, Numerical simulation of riblet controlled spatial transition in a zero-pressure-gradient boundary layer, Flow, Turbulence and Combustion, 85 (1), 57–71, DOI:10.1007/s10494-010-9251-x.
Klumpp S., Guldner T., Meinke M., Schroder W., 2010, Riblets in a turbulent adverse-pressure gradient boundary layer, AIAA 5th Flow Control Conference, AIAA 2010-4706, DOI: 10.2514/6.2010-4706.
Kurita M., Iijima H., Koga S., Nishizawa A., Kwak D., Iijima Y., Takahashi H., Abe H, 2020, Flight test for paint-riblet, AIAA Scitech 2020 Forum, DOI:10.2514/6.2020-0560.
McLean J., George-Falvey D., Sullivan P., 1987, Flight test of turbulent skin-friction reduction by riblets, International Conference on Turbulent Drag Reduction by Passive Means, 408–448.
Mele B., Tognaccini R., 2012, Numerical simulation of riblets on airfoils and wings, 50th AIAA Aerospace Sciences Meeting including the New Horizons Forum and Aerospace Exposition, AIAA 2012-861, DOI:10.2514/6.2012-861.
Mele B., Tognaccini R., 2018, Slip length-based boundary condition for modeling drag reduction devices, AIAA Journal, 56 (9), 3478–3490, DOI:10.2514/1.J056589.
Viswanath P., 2002, Aircraft viscous drag reduction using riblets, Progress in Aerospace Sciences, 38 (6–7), 571–600, DOI:10.1016/S0376-0421(02)00048-9.
Walsh, M., Anders J., 1989, Riblet/LEBU research at NASA Langley, Applied Scientific Research, 46 (3), 255–262, DOI:10.1007/BF00404822.
Walsh M., Sellers I., McGinley C., 1989, Riblet drag reduction at flight conditions, Journal of Aircraft, 26 (6), 570–575, DOI:10.2514/6.1988-2554.
Zhang Y., Chen H., Fu S., Dong W., 2018, Numerical study of an airfoil with riblets installed based on large eddy simulation, Aerospace Science and Technology, 78, 661–670, DOI:10.1016/j.ast.2018.05.013.